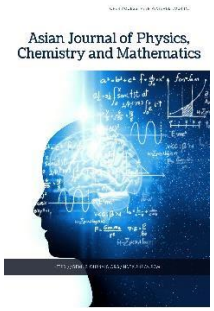

On the short period evolution of Third body perturbation on Low Earth Orbit (LEO) satellite

Mustafa Najat Kareem[1] Department of physics- college of Science - University of kirkuk – Kirkuk-Iraq . Email mustafanajat@uokirkuk.edu.iq

Wafaa Hasan ali zaki[2] Department of physics- college of Science - University of kirkuk – Kirkuk-Iraq . Email: wafaa_1966@uokirkuk.edu.iq

Ahmed Kader Izzet[3] Northern technical university / engineering technical college / Kirkuk-Iraq. Email : ahmed_izeet@ntu.edu.iq

ABSTRACT

A sun-synchronous orbit, sometimes called an helio-synchronous orbit, is when the Earth orbits the sun at a constant angle relative to the Earth-sun direction. In this work, the analytical technique for third body perturbation on sun-synchronous orbit satellites for prograde and retrograde orbits computed for short periods At a time interval of one day, the dynamic development of sun-synchronous orbits is considered. It was accomplished by utilizing the numerical output results from the celestial mechanics' version 1 software program package. The integration was carried out by using the Celestial Mechanics software program SATORB module (Beutler, 2005) created at the University of Bern's Institute of Astronomy. With input data given by the Two-Line Elements (TLE). Represented by six orbital elements and three Coordinates axes and acceleration components which were used to solve the variation of parameters equations (VOP) using a technique known as collocation method. It is reasonable to assume that the change in orbital elements is seen in both types of perturbations that have the greatest impact on the moon's impact. With the addition of the Geocentric equatorial coordinate system, Kepler's orbit, and acceleration combinations, there was no discernible change in the coordinate system or acceleration components, which appeared to be secular in both results. The results show that the Moon perturbation has the greatest influence on orbital elements and that the perturbation is amplified by satellite heights.

Keywords: Third body perturbation; Low orbits satellites; Retrograde and programed orbits; Orbital elements.

1- Introduction

The Meteor-M spacecraft series is being developed as a prime contractor for Roskosmos by RSC (Research and Production Corporation) VNIIEM in Moscow. Each satellite in the series weighs 2,800 kg, including 1,250 kg for the satellites' multi-instrument payload suite. While the Meteor-M satellites share several instruments, some are unique to each spacecraft to increase the available data [1]. In astrodynamics, studying and modeling perturbations are important fields. Even though the majority of the solution approaches have been around for a long time, Perturbations are motions that deviate from a normal, idealized, or unaltered state. We tend to think of the cosmos as being quite regular and predictable. However, good observational data frequently exposes inexplicable anomalies of motion overlaid on the celestial bodies' more regular or mean movements [2]. Although the exact location of a

low Earth orbit is unclear, it is generally thought to be between 100 and 1000 kilometers above the Earth's surface. This is the most cost-effective and straightforward orbit for a spacecraft to enter. Getting a spacecraft into a low-earth orbit (LEO) uses less energy than getting it into a higher-altitude orbit [3]. Due to the impact of numerous "disturbing" factors, a satellite's real orbit deviates from the Keplerian orbit. This includes, among other things, the Earth's non-spherical gravity, the gravitational influences of the moon and sun, atmospheric air drag, and solar radiation pressure. These disrupting forces produce temporal changes in the orbital elements of secular, long- and short-periodic nature (orbital perturbations). The real orbit can be thought of as the envelope of Keplerian ellipses provided by the actual orbital components at any given time (osculating ellipses). Artificial Earth satellites have been used for geodetic applications such as locating and determining the Earth's gravitational field and rotation characteristics since the launch of Sputnik I in 1957. Only a few satellite missions have been specifically intended for geodetic purposes. However, geodesy makes considerable use of a vast number of satellites produced for navigation, remote sensing, and geophysics [4]. The satellite motion is called prograde motion when the inclination is between 0 and 90 degrees. Retrograde motion is defined as motion that is oriented westward for inclinations between 90 and 180 degrees [5]. Satellites are attracted not just by the Earth's central force, but also by its non-central force, the sun and moon's attractive forces, and the drag force of the atmosphere. Solar radiation pressure, Earth and ocean tides, general relativity effects, and coordinate perturbations all have an impact on them. Satellite motion equations must be expressed using perturbed equations [6]. Third body perturbation has a long time of study and investigations with many research and papers concluding different subjects working with this topic these as an example for this study is Kozai Yoshihide (1959), the current article deduces as a function of mean orbital elements and time perturbations of six orbital elements of a near-earth satellite passing through the earth's gravitational field without meeting air resistance. No assumptions are made about the degree of eccentricity or inclination [7]. According to Kozai Yoshihide (1973) this paper pioneered an entirely new approach for computing lunisolar perturbations. The disturbing function is defined as the satellite's orbital components and the sun and moon's polar coordinates [8]. Lara M. (2012) used perturbation theory based on Lie transformations and higher-order averaging to investigate the long-term evolution of GNSS-type orbits[9]. Roscoe W.T.C. (2015) studied the impact of lunisolar perturbation on a satellite by utilizing differential orbital elements to express the relative velocity of the satellite in absolute and differential terms [10]. B. Saedeleer (2006) The analytical theory of the Moon's third body, was studied using the Lie transform method for averaging Hamiltonians in cases of synchronous rotation, the Lunar oblateness, the Lunar triaxiality, and the significant influence of the Earth's lunisolar rotation (ELP 2000) [11]. According to Beutler (2006), the paper discusses the development of effective methods for predicting the orbits of low-earth-orbiting objects (LEOs) in the presence of imprecisely characterized force fields. Pseudo-stochastic pulses, piecewise constant accelerations, or piecewise linear and continuous accelerations are used to compensate for the force field's deficiencies [12]. Xua Guangyan, Luo Jianfu and others (2014) Using the Reference Satellite Variable, this paper derives equations for low earth satellites and their relative motion under lunar perturbation (RSV). The derivation incorporates some plausible assumptions to simplify the results and emphasize the third body's influence [13]. Kuznetsov E. D. and Jasim A. T. This study examines the dynamic evolution of sun-synchronous orbits during a time range of 20 years. The dynamic evolution of two families of sun-synchronous orbits with altitudes of 751 and 1191 km is explored about the starting value of the ascending node longitude. Numerical motion simulations were performed using the Celestial Mechanics software program created at the University of Bern's Institute of Astronomy [14]. Ahmed K. Izzet and others (2019) The primary purpose of this study is to calculate the tide effect perturbations on LEO satellites. This, adjustments in the orbital elements must be

made. These elements stay constant in the absence of perturbations. The results indicate that tidal disturbance's influence on orbital elements depends on the satellite orbit's inclination. The variance in the ratio diminishes as the inclination of the satellite increases but increases as the period grow [15]. Chihabi Yazan and Ulrich Steve (2021) Using conventional orbital components, this article presents an analytical solution for the relative velocity of two spacecraft. The analytical solution is obtained by forward propagating the orbital elements in time and accounting for gravitational field perturbations up to the fifth harmonic, third-body, and drag secular and periodic perturbations and calculating the relative motion in the local-vertical–local-horizontal reference frame at each time step. Compared to a numerical simulator, the analytical solution accurately characterized the relative motion, with errors on the order of meters at separation distances of hundreds of meters [16]. Dua Yujun and Zhang Fangzhao (2021): Theoretically and numerically, we explore these effects using Gaussian equations of motion. According to the study, PNPM's effect may be classified into two groups. The first component is a rotational error in the perturbing force vector caused by the force vector being converted to a coordinate system without accounting for PNPM effects; the second component is an error in the satellite coordinates computed in the Earth-Centered Earth-Fixed (ECEF) or True-of-Date (TOD) coordinate system without accounting for PNPM effects. Additionally, a straightforward semi-analytical correction strategy is shown. Keplerian elements can be employed instantly without requiring a recalculation of the solutions. This method effectively corrects the error produced when the PNPM was disregarded [17]. Ahmed K. Izzet and others (2019) The primary purpose of this study is to calculate the tide effect perturbations on LEO satellites. This, adjustments in the orbital elements must be made. These elements stay constant in the absence of perturbations. The results indicate that tidal disturbance's influence on orbital elements depends on the satellite orbit's inclination. The variance in the ratio diminishes as the inclination of the satellite increases but increases as the period grow [15]. Najlaa Ozaar Hasan and others (2021): The research was divided into two sections; the first examines the effects of air drag on various area-to-mass ratios of LEO satellites, while the second examines various inclination values. Each component includes a section on modeling perturbation effects, and the last section examines the effects of air drag at various node values. The simulation was conducted using the SATORB module of the Celestial Mechanics software system (Beutler, 2005). The results indicate that the impacts are stronger for retrograde orbits since the satellite travels in the opposite direction. The atmospheric drag effects were amplified by raising the area to mass ratio of all orbital components. When the value of a node increases [18]. Elisa Maria Alessi, Alberto Buzzoni and others (2021). The purpose of this study is to evaluate the orbital development of the mean eccentricity as defined by the Molniya satellites constellation's Two-Line Elements (TLE) set. The bottom-up technique is used to achieve synergy between observable dynamics and mathematical simulation. With the long-term development of eccentricity as the primary emphasis, the dynamical model used is a doubly-averaged formulation of the third-body disturbance caused by the Sun and Moon and the oblateness influence on the satellite's orientation. The findings demonstrate that the second-order expansion captures the behavior remarkably well despite the very elliptical orbits. Additionally, the lunisolar influence is not negligible for the behavior of the ascending node's longitude and the pericenter's argument. Finally, a frequency series analysis is suggested in order to demonstrate [19]. Dua Yujun and Zhang Fangzhao (2021) Theoretically and numerically, we explore these effects using Gaussian equations of motion. According to the study, PNPM's effect may be classified into two groups. The first component is a rotational error in the perturbing force vector caused by the force vector being converted to a coordinate system without accounting for PNPM effects; the second component is an error in the satellite coordinates computed in the Earth-Centered Earth-Fixed (ECEF) or True-of-Date (TOD) coordinate system without accounting for PNPM effects.

Additionally, a straightforward semi-analytical correction strategy is shown. Keplerian elements can be employed instantly without requiring a recalculation of the solutions. This method effectively corrects the error produced when the PNPM was disregarded [17].

This study aims to analyze the third body perturbation of the Low Earth orbit METEOR-M satellite for prograde and retrograde orbits using celestial mechanics software program version one. Additionally the study demonstrate that how it impacts orbital elements, Geocentric equatorial Coordinates system, kepler's orbit and components of acceleration during one day.

2. Sun-synchronous orbit

Sun-synchronous orbits in which the ascending node's secular rate of right ascension is equal to the mean sun's right ascension rate. To be sun-synchronous, the inclination, semi-major axis, and eccentricity of the satellite orbit. A typical sun-synchronous orbit has an inclination of 98.7 degrees and a mean orbit height of 833 kilometers. Circular orbits at low height [20].

$$\left(\frac{d\Omega}{dt}\right)_s = -\frac{3}{2} n J_2 \left(\frac{R}{P}\right)^2 \cos i = 0.9856 \ \frac{deg}{day}$$

Where

$n = \sqrt{\frac{\mu}{a^3}}$ orbit mean motion

R = Earth equatorial radius

$p = a(1 - e^2)$

3. Simulation of satellite motion in Sun-synchronous satellite via numerical models

The motion of Sun-synchronous near-circular orbit, mean altitude of 7195 km, inclination = 98.85° and 1.71° with period of 101.3 minutes, local equatorial crossing time at 12:00 hours. Significant perturbing factors, such as the Moon's and Sun's pull, were considered. The perturbing bodies' coordinates were obtained using numerical ephemerides DE200/LE200). Using the Celestial Mechanics software system's SATORB module (Beutler, 2005). Since the integration is performed over a short time period and no connection to individual data is required, the beginning epoch of September 17, 2009, was chosen for ease of use of the numerical model. The integration was done using the 12th order collocation approach with integration order of 12 and automatic step selection 607.2 seconds in one day of age with tabular interval of 0.1. The model used in this process which is Joint Gravity model (JGM3) the JGM model was developed with NASA and the university of Texas in 1994 [21][22].

4. Perturbation due to third body

The equations of motion of two point masses M and m when they interact are as follows

$$M\ddot{\vec{r}}_M = GMm\frac{\vec{r}_{Mm}}{r_{Mm}^3} \quad and \quad m\ddot{\vec{r}}_m = GMm\frac{\vec{r}_{mM}}{r_{mM}^3} \ \ldots (1)$$

Where r is the vector's length, index Mm indicates that the vector points from point-mass M to point-mass m and single index M or m indicates that the vector points to point-mass M or m. By introducing additional point masses m(j), j = 1, 2,..., the attraction of m(j) on M and m may be expressed, and summations can calculate the total attraction [23].

$$M\ddot{\vec{r}}_M = GM_m\frac{\vec{r}_{Mm}}{r_{mM}^3} + \sum_j GMm(j)\frac{\vec{r}_{Mm(j)}}{r_{Mm(j)}^3}$$

$$m\ddot{\vec{r}}_m = GMm\frac{\vec{r}_{mM}}{r_{mM}^3} + \sum_j Gmm(j)\frac{\vec{r}_{mm(j)}}{r_{mm(j)}^3}$$

By dividing the two preceding equations by $-M$ and m and then adding them together, one obtains

$$\ddot{\vec{r}}_m - \ddot{\vec{r}}_M = -G(M+m)\frac{\vec{r}_{Mm}}{r_{mM}^3} + \sum_j Gm(j)\left\{\frac{\vec{r}_{mm(j)}}{r_{mM}^3} - \frac{\vec{r}_{Mm(j)}}{r_{Mm(j)}^3}\right\} \ldots (2)$$

Letting $\vec{r} = \vec{r}_m - \vec{r}_M$ using the point mass (M) as the origin substituting $\vec{r}_{mm(j)} = -(\vec{r}_m - r_{m(j)})$ in the right side of equation (2) and removing the mass m (mass of satellite)

$$\ddot{\vec{r}} = -GM\frac{\vec{r}}{r^3} - \sum_j Gm(j)\left\{\frac{\vec{r}-\vec{r}_{m(j)}}{\left|\vec{r}-\vec{r}_{m(j)}\right|^3} + \frac{r_{m(j)}}{r^3_{m(j)}}\right\} \ldots\ldots (3)$$

It is self-evident that the first component on the right represents the earth's core force; hence, the disturbance forces of various point masses acting on the satellite are then calculated.

$$\vec{f}_m = -m\sum_j Gm(j)\left\{\frac{\vec{r}-\vec{r}_{m(j)}}{\left|\vec{r}-\vec{r}_{m(j)}\right|^3} + \frac{\vec{r}_m}{r^3_{m(j)}}\right\} \ldots (4)$$

Where Gm(j) denotes the sun, moon, and planets' gravitational constants [23].

5. Collocation method

The collocation approach is used to solve the problem of starting value. Collocation algorithms use a polynomial of degree q to estimate the initial value issue inside the subintervals I_k, which is (in general) greater than Euler's approach. (The collocation algorithm is simplified to the Euler algorithm for q = n.) The order of the technique is also known as the polynomial degree $q \geq n$. The problem with the interval as the starting value may be stated as:

$$y_k^{(n)} = f(t, y_k, \dot{y}_k, \ldots, y_k^{(n-1)})$$

$$y_k^{(i)}(t_k) = y_{k0}^{(i)} \quad i = 0, 1, \ldots, n-1$$

Where $y_{k0}^{(i)}$ is initial value

The collocation algorithm of order $q \geq n$ uses a polynomial of degree q to approximate the initial value issue or the boundary value problem in the interval $I_k = [I_k, t_k + 1]$.

$$y_k(t) = \sum_l^q \frac{1}{l!}(t-t_k)^l \; y_{k0}^{(l)} \ldots\ldots (5)$$

Within the interval I_k, the differential equation system was solved by numerical solution at exactly $q + 1 - n$ distinct epochs t_{k_j} , $j = 1, 2, \ldots, q + 1 - n$

6. Conservative Forces Lagrangian (VOP)

The VOP technique is well-suited for generating the equations of motion of perturbed dynamical systems. The concept is founded on the assumption that if the solution's constants are extended to be time-varying parameters, we may utilize the unperturbed system to represent the solution to the perturbed system. The unperturbed system is a two-body system that consists of a series of formulae for determining the position and velocity vectors at a given time. Bear in mind that these computations depend on the six orbital components and time. We may theoretically employ any set of unchanged motion constants, including the original position and velocity vectors. Time is related to motion equations via mean, eccentric, and actual anomaly conversions. The Lagrangian planetary equations of motion, or simply the Lagrangian VOP, are the essential theory for calculating the orbital components' rates of change. It is named after Lagrange since he is credited with formulating these equations for the first time for all six orbital elements. He was mesmerized by the minute perturbations of planets' orbits around the Sun caused by their gravitational attraction [24].

The planetary equation of Lagrange for the orbit of a celestial body in a two-body situation is stated as [22].

$$\dot{a} = \mp\frac{2}{n^2 a}\frac{\partial R}{\partial \dot{T}_0} \ldots\ldots\ldots\ldots (6)$$

$$\dot{e} = -\frac{\sqrt{|1-e^2|}}{n\,a^2 e}\frac{\partial R}{\partial \omega} - \frac{1-e^2}{n^2 a^2 e}\frac{\partial R}{\partial \dot{T}_0} \ldots (7)$$

$$\frac{di}{dt} = -\frac{1}{n\,a^2\sqrt{|1-e^2|}\sin i}\frac{\partial R}{\partial \Omega} + \frac{\cot i}{n\,a^2\sqrt{|1-e^2|}}\frac{\partial R}{\partial \dot{T}_0} \ldots (8)$$

$$\dot{\Omega} = \frac{1}{na^2\sqrt{|1-e^2|}\sin i}\frac{\partial R}{\partial i} \ldots\ldots\ldots\ldots (9)$$

$$\dot{\omega} = \frac{\sqrt{|1-e^2|}}{n\,a^2 e}\frac{\partial R}{\partial e} - \frac{\cot i}{n\,a^2\sqrt{|1-e^2|}}\frac{\partial R}{\partial i} \ldots (10)$$

$$\dot{T}_0 = \frac{2}{n^2 a}\frac{\partial \dot{R}}{\partial a} + \frac{1-e^2}{n^2 a^2 a}\frac{\partial R}{\partial e} \ldots\ldots\ldots\ldots (11)$$

7. Non-conservative forces Gaussian form

It is sometimes more convenient to represent disturbing accelerations directly at the satellite in componential form rather than using partial derivatives of the disturbing potential in the elements. This is especially true for orbits with a large eccentricity, for which series expansions would need a large number of terms in e. Gauss proposed a feasible alternative form. Three mutually perpendicular components are used to resolve the perturbing forces operating on the satellite [24].

As an example, consider the following collection of Gaussian perturbation equations to reduce (RSW) [22].

$$\dot{a} = \sqrt{\frac{p}{\mu}}\,\frac{2a}{1-e^2}\left\{e\sin v R + \frac{p}{r}S\right\} \ldots\ldots (12)$$

$$\dot{e} = \sqrt{\frac{p}{\mu}}\,\{\sin v\, R + (\cos v + \cos E)\, S\} \ldots\ldots (13)$$

$$\frac{di}{dt} = \frac{r\cos u}{n\,a^2}\,W \ldots\ldots\ldots\ldots\ldots\ldots (14)$$

$$\dot{\Omega} = \frac{r\sin u}{n\,a^2\sqrt{1-e^2}\,\sin i}\,W \ldots\ldots\ldots\ldots (15)$$

$$\dot{\omega} = \frac{1}{e}\sqrt{\frac{p}{\mu}}\left\{-\cos v\, R + \left(1+\frac{r}{p}\right)\sin v\, S\right\} - \cos i\,\dot{\Omega} \ldots\ldots (16)$$

$$\dot{T}_0 = -\frac{1-e^2}{n^2\,ae}\left\{\left(\cos v - 2e\frac{r}{p}\right)R - \left(1+\frac{r}{p}\right)\sin v\, S\right\} - \frac{3}{2a}\left(t - \dot{T_o}\right)\dot{a} \ldots\ldots (17)$$

Where v is true anomaly, E is eccentric anomaly and $u = \omega + v$ is the argument of latitude of the celestial body. The perturbation equations above are divided into two groups, the first of which contains the equations for the semimajor axis a (which defines the size), the eccentricity e (which defines the shape), and the time T0 of pericenter passage (which defines the dynamics) of the orbital motion, and the second of which contains the three Eulerian angles I and, which define the orbital plane and the orientation of the conic section within it [25].

8. Results and discussion

(a)

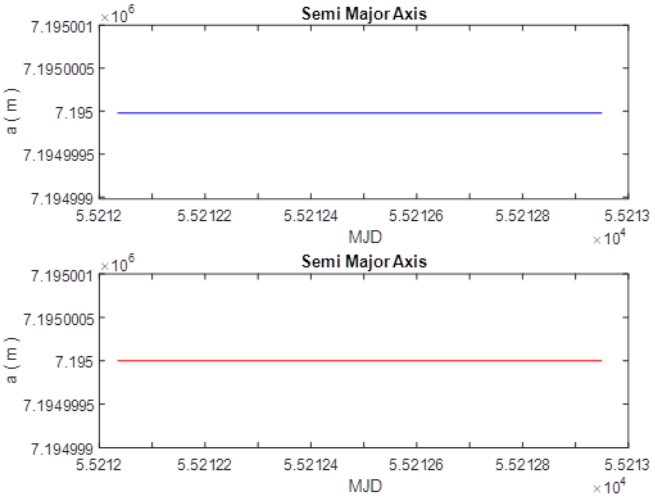

(b)

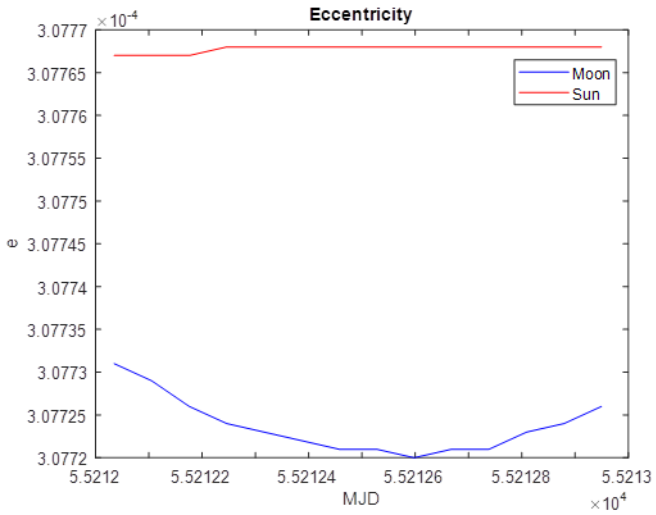

(c)

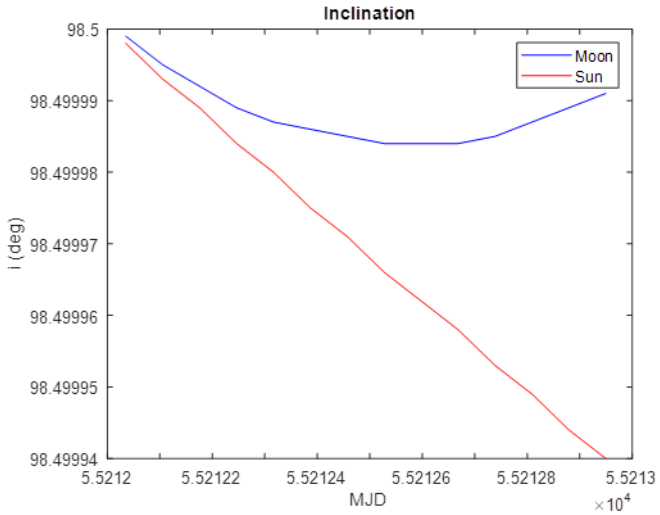

(d)

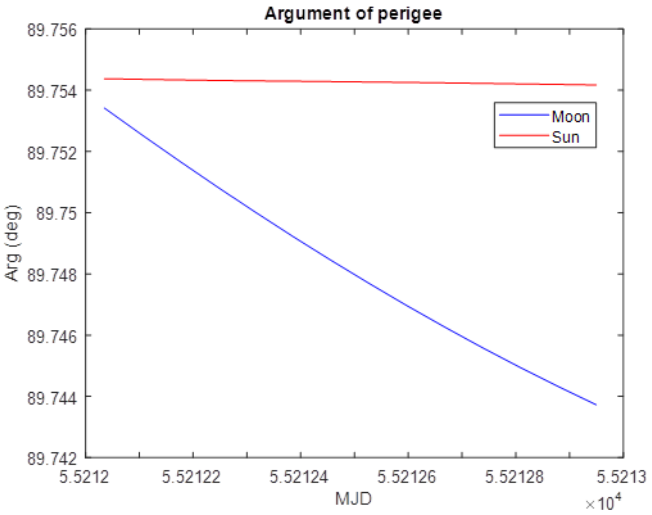

(f)

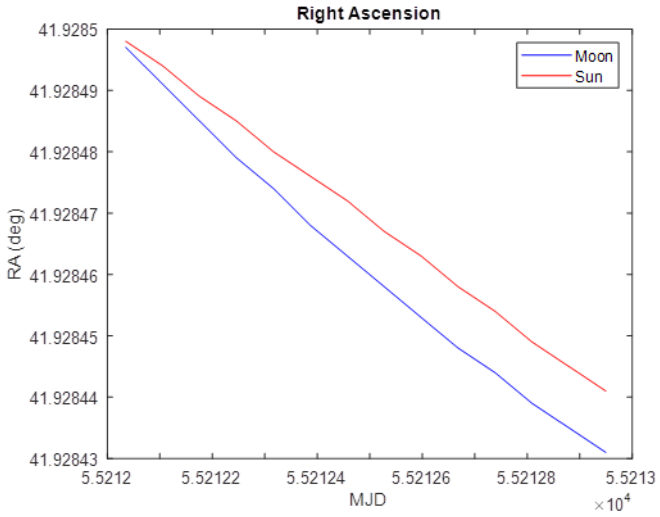

(e)

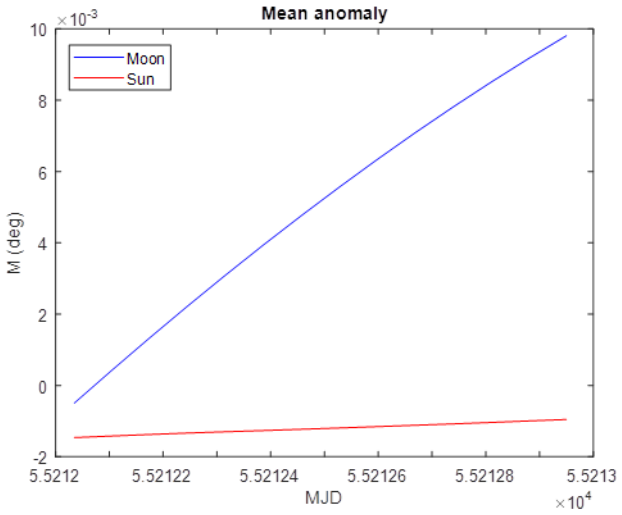

Figure 1: Orbital elements under the influence of Third body perturbation for retrograde Low Earth Orbit satellite (LEO). Where (a) denotes the Semi Major axis, (b) denotes eccentricity, (c) denotes inclination, (d) denotes right ascension, (e) denotes perigee argument, and (f) denotes mean anomaly.

(a)

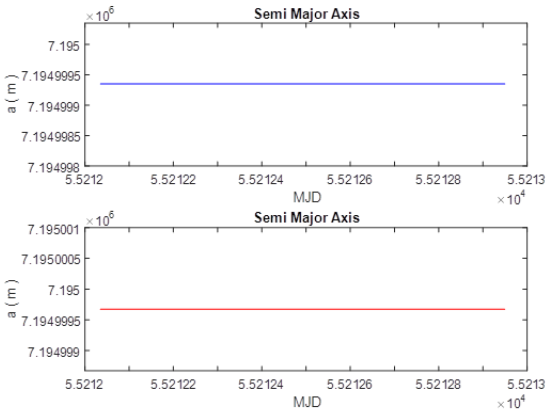

(b)

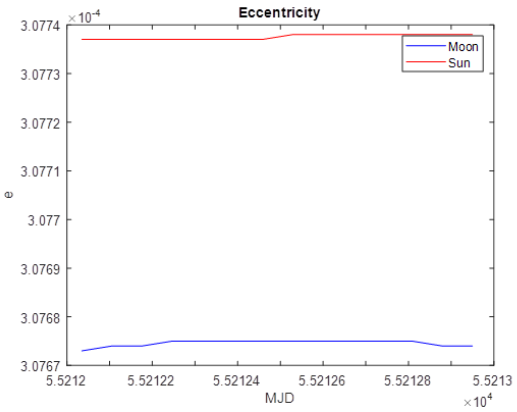

(c)

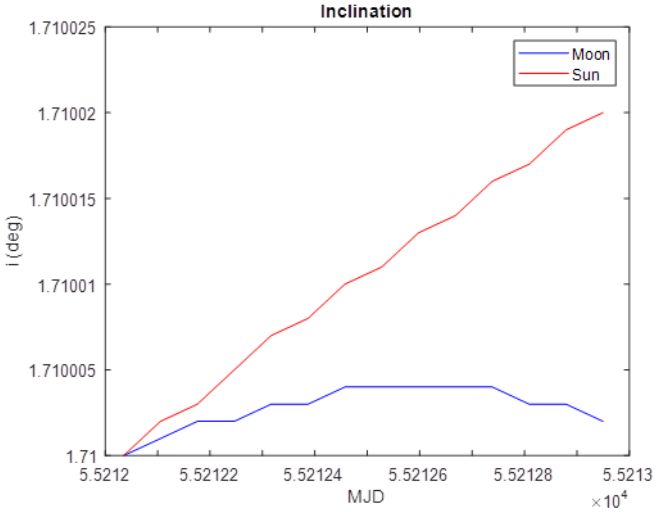

(d)

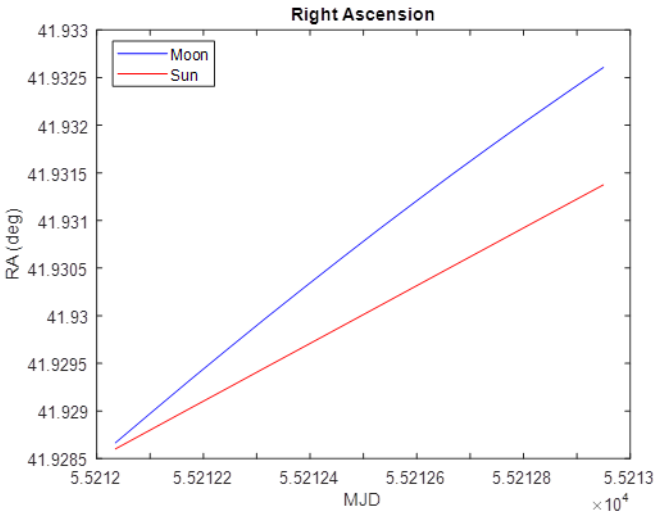

(e)

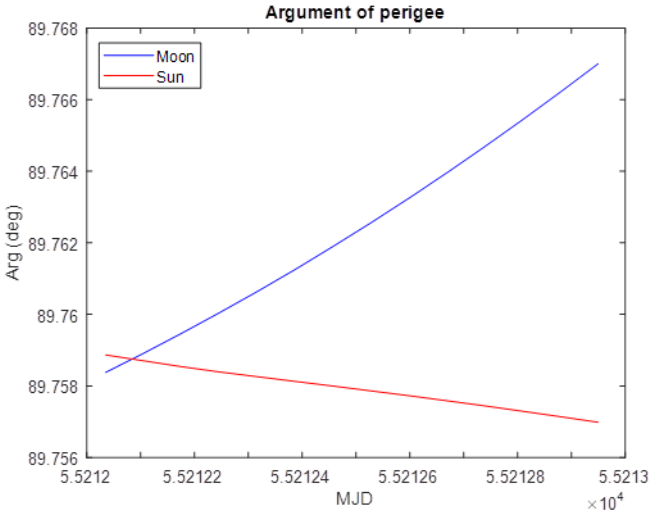

(f)

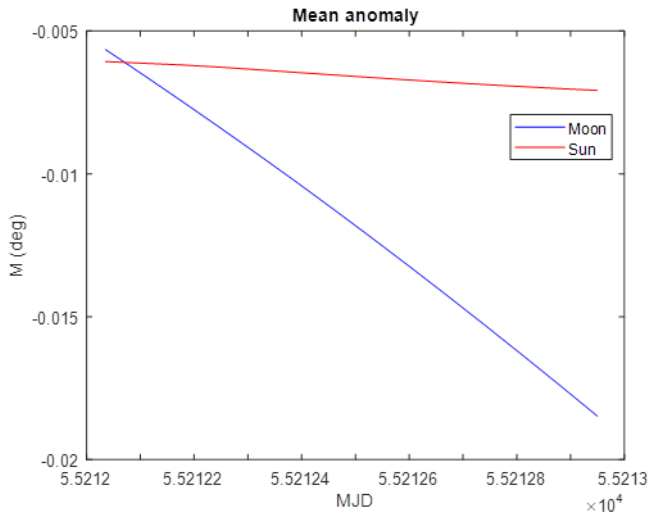

Figure 2: Orbital elements under the influence of Third body perturbation for prograde Low Earth (LEO) satellite.

Figure (1) and (2) depict the effect of third-body perturbation (Moon, Sun) on orbital elements for LEO satellites in retrograde and prograde orbits. As shown in the figures, the elements (RA, Arg and Mean anomaly) are more affected by the Moon than the Sun, while the inclination of the satellite is much more affected by Sun gravitation than that caused by the Moon. The semi-major axis (a) and eccentricity (e), which govern the size and shape of the orbits, respectively is unaffected by the third body

perturbation. As in the figures, the three Eulerian angles I, RA, and Arg) decrease for retrograde orbits while increasing for prograde orbits. The shift in Mean anomaly also rises for retrograde orbits while decreasing for prograde orbits.

(a)

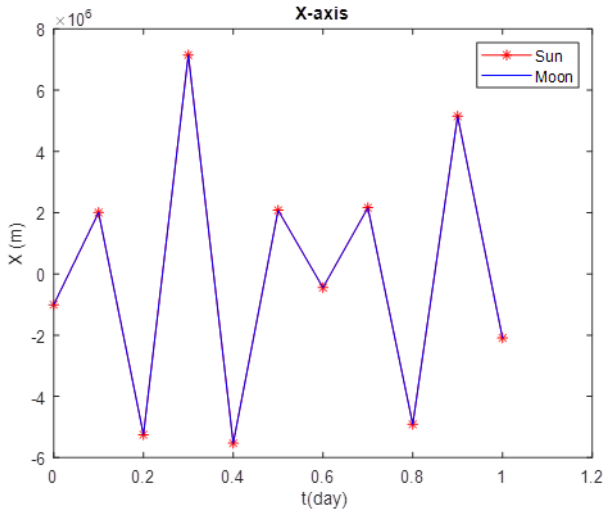

(b)

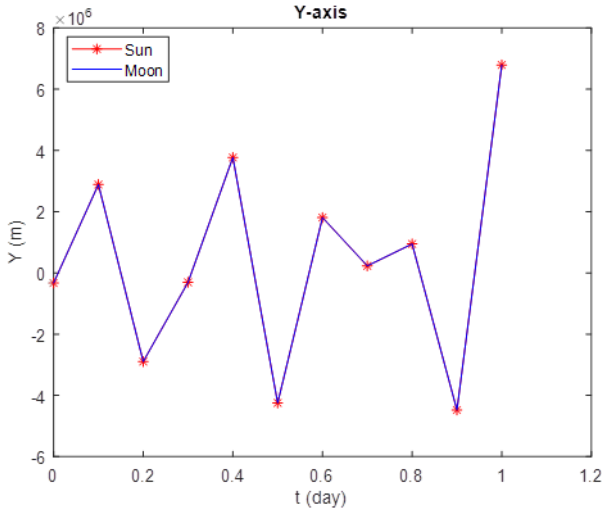

(c)

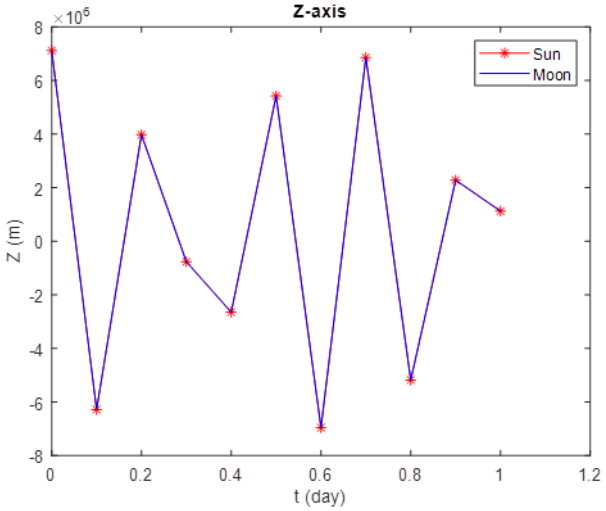

(d)

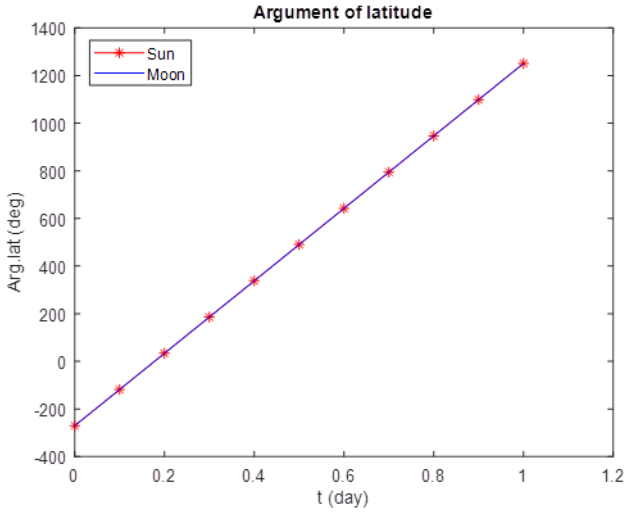

(e)

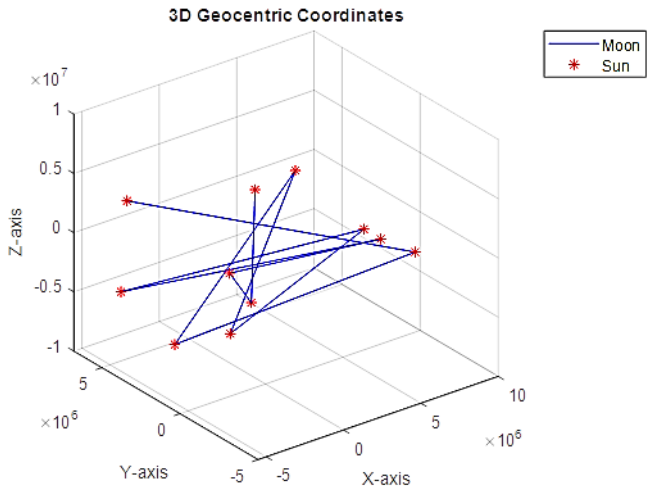

Figure (3): Geocentric equatorial coordinates under Third body perturbation for retrograde Low Earth Orbit (LEO) Satellite Where: (a) represent X-axis, (b) Y-axis, (c) Z-axis, (d) Argument of latitude, and (e) Coordinates in 3D.

(a)

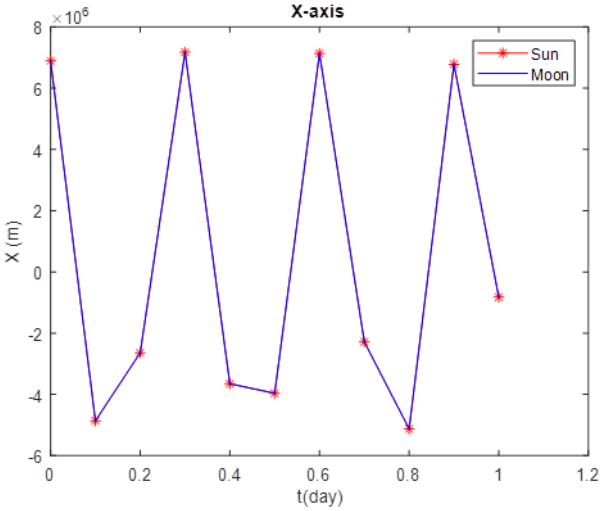

(b)

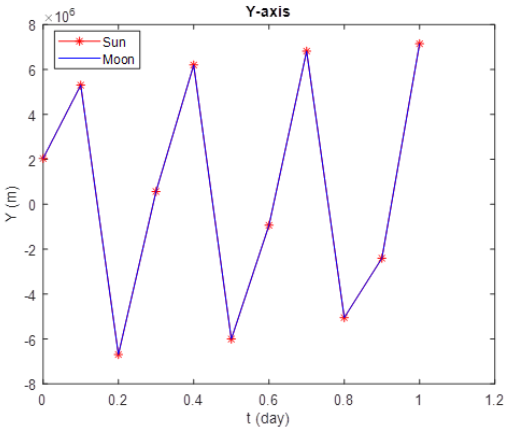

(c)

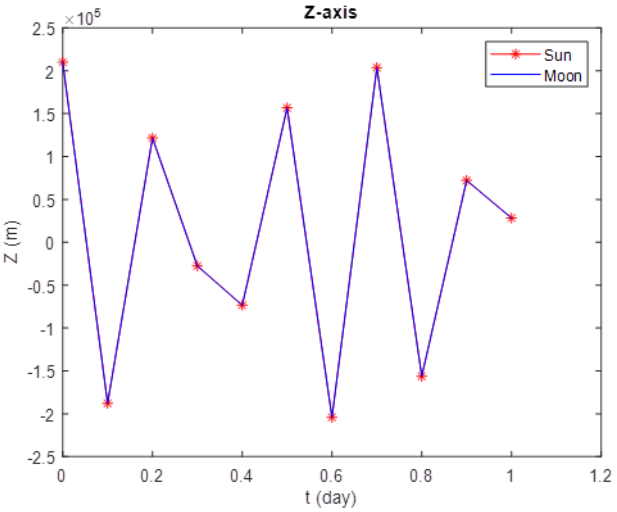

(d)

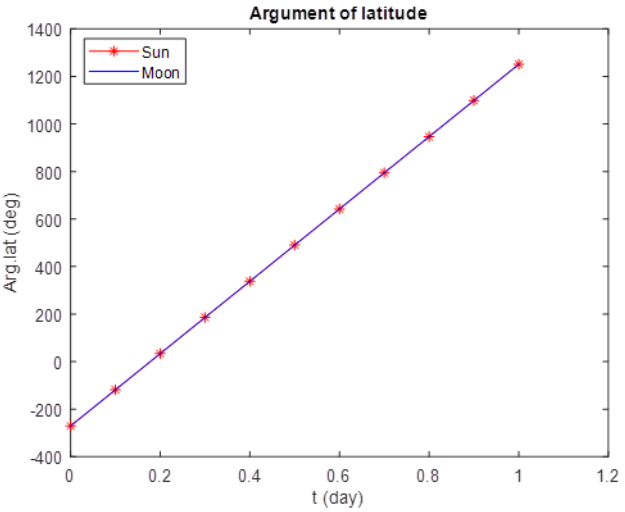

(e)

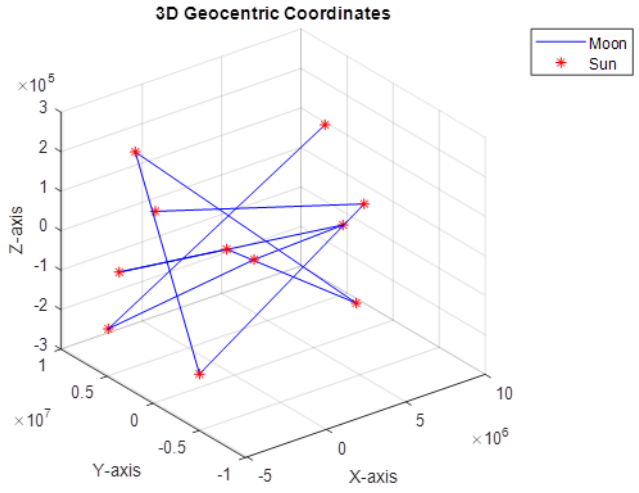

Figure (4): Geocentric equatorial coordinates under third body perturbation for prograde Low Earth orbit (LEO) satellite.

As shown in figures (3) and (4), the research also covers the portion of perturbation on Geocentric equatorial coordinates (X, Y and Z). The results indicated that the impacts of the Sun and Moon perturbations on low–altitude satellites are equal and periodic but with a great range of influence for both retrograde and prograde orbits, and this assessment also applies to the argument of latitude.

(a)

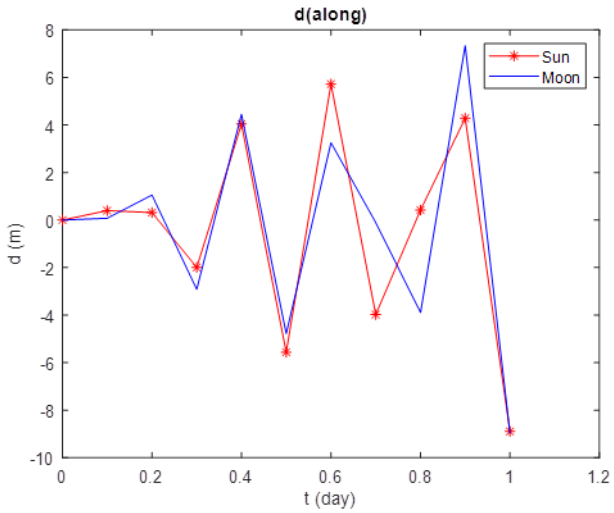

(b)

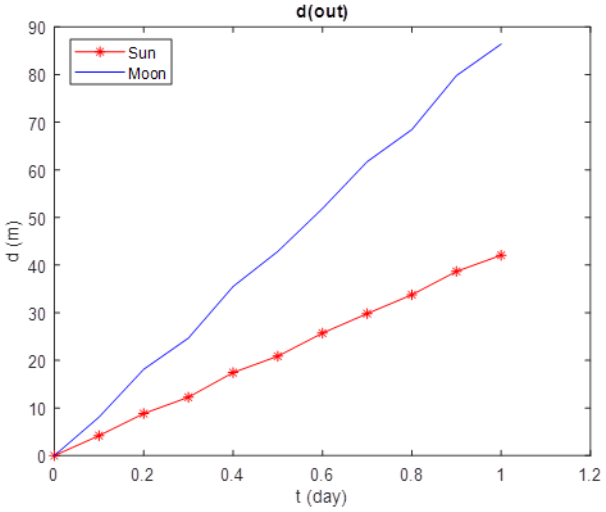

(c)

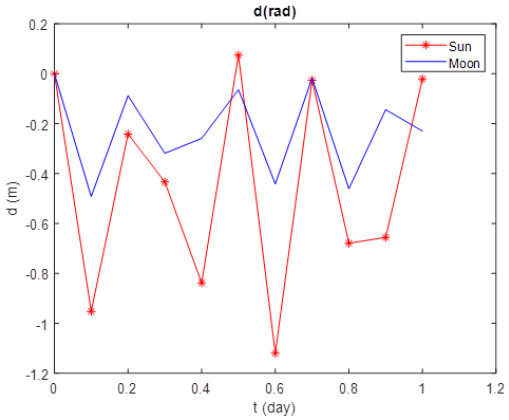

(d)

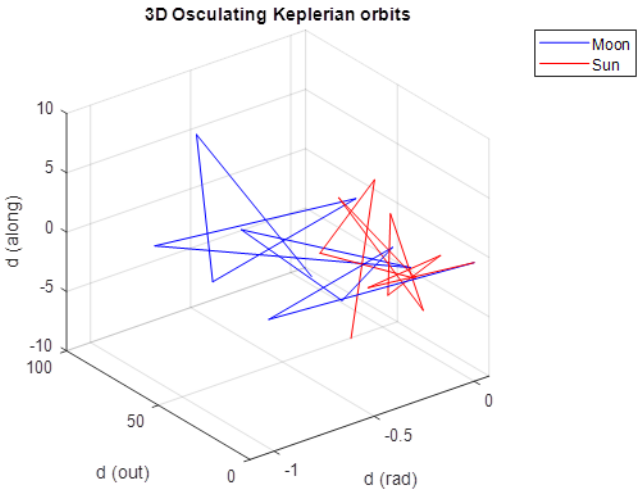

Figure (5): Keplerian orbit during perturbation on retrograde Low Earth Orbit satellite (LEO). Where: (a) represent radial, (b) along-track, (c) out of plane and (d)

acceleration components in 3D.

(a)

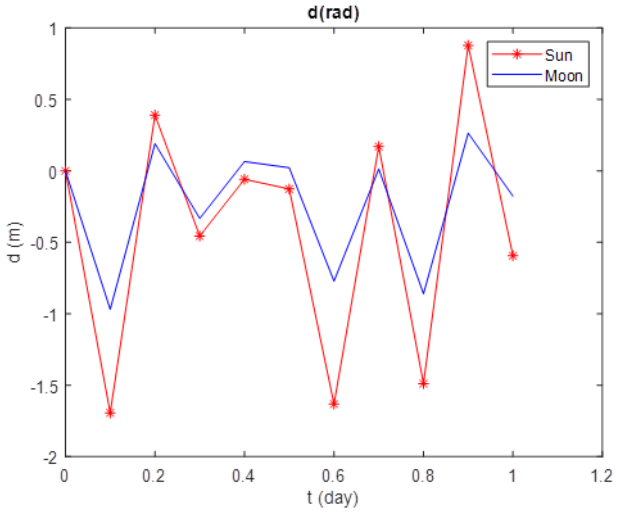

(b)

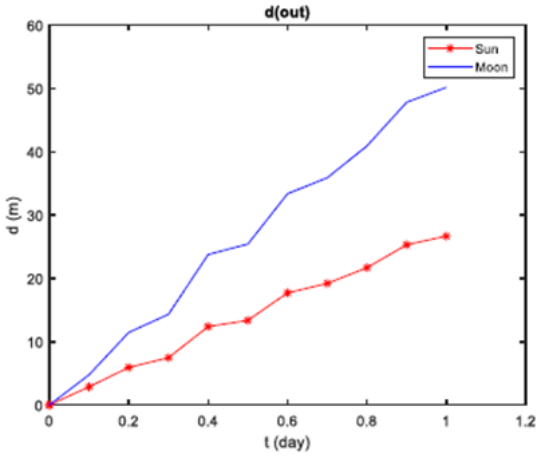

(c)

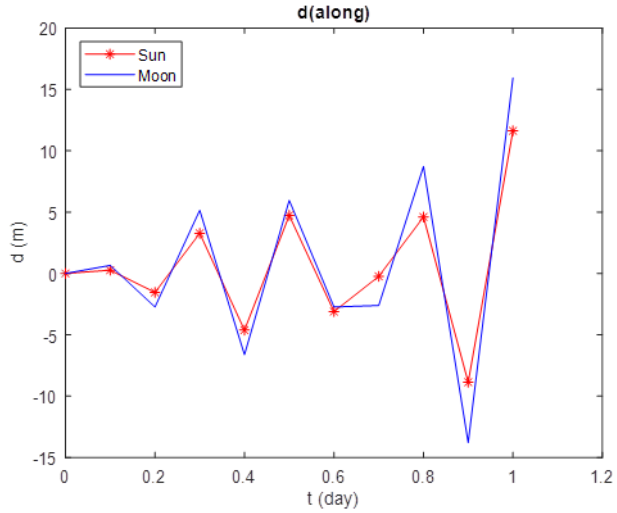

(d)

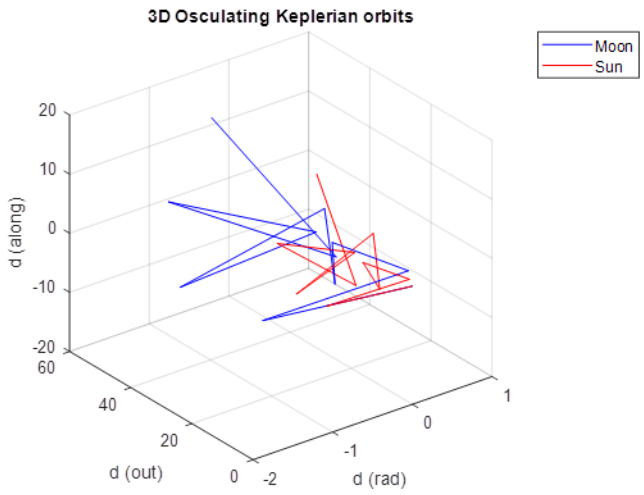

Figure (6): Keplerian orbit during perturbation on prograde Low Earth Orbit satellite (LEO).

Figures (5) and (6) illustrate the changes in radial, along-track, and out-of-plane directions of the perturbed orbits about the osculating orbits. in figure (5) the radial direction has small and periodic effect with highest influence of Sun perturbation, and in the out of plane the rate of perturbation increasing with time and have greatest effect of Moon at point equal to $\mathbf{90}\,\boldsymbol{m}$ and at $\approx \mathbf{40}\,\boldsymbol{m}$ for Sun effect. In figure (6) the radial direction which has short period effect with highest effect for Sun, the out of plane has increasing rate of change with increasing the period of time with maximum influence at $\mathbf{50}\,\boldsymbol{m}$ for Moon effect and at $\mathbf{25}\,\boldsymbol{m}$ for Sun effect. Prograde orbits have a higher difference in radial and along direction than retrograde orbits, while the difference in out-of-plane direction is greater in retrograde. The sun has a stronger radial influence than the moon, whereas the moon has a more significant out-of-plane effect. In total high effect is recognized in sections of out of plane and along direction.

(a)

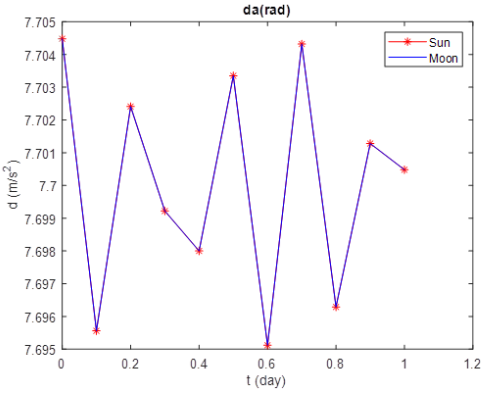

(b)

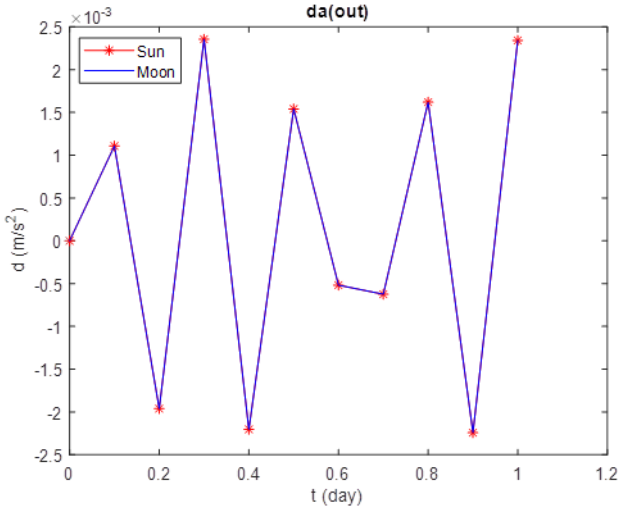

(c)

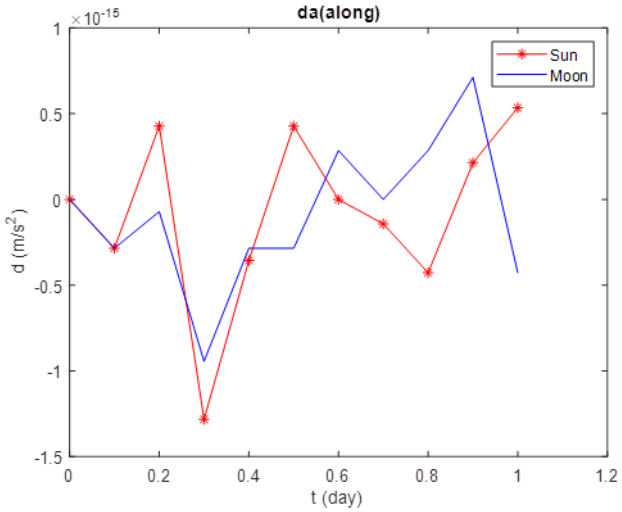

(d)

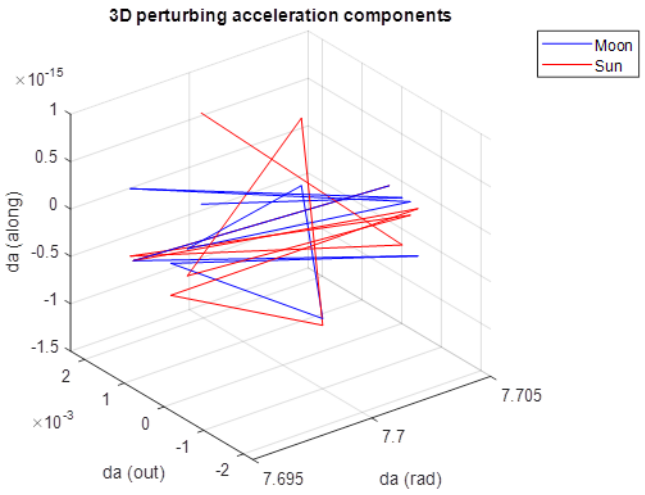

Figure (7): Acceleration components directions during perturbation on retrograde Low Earth Orbit (LEO) satellite. Where: (a) represent radial, (b) along-track, (c) out of plane and (d) acceleration components in 3D.

(a)

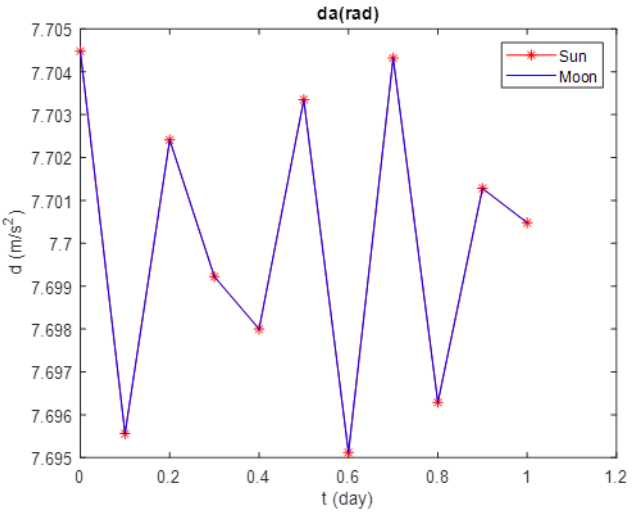

(b)

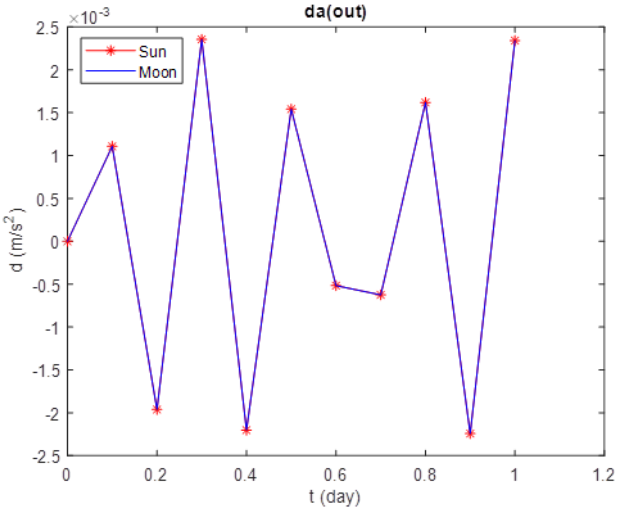

(c)

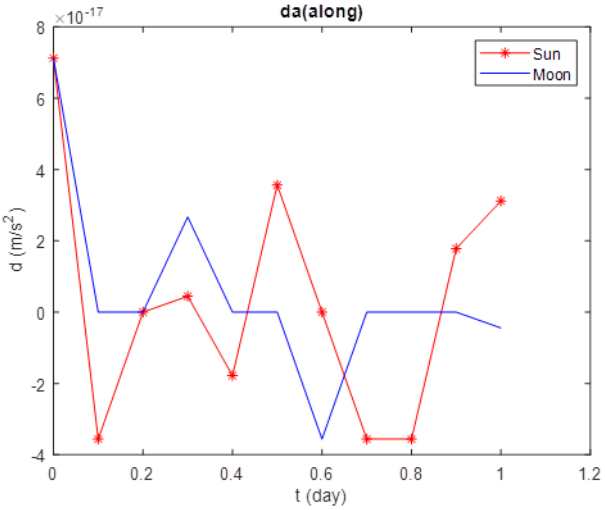

(d)

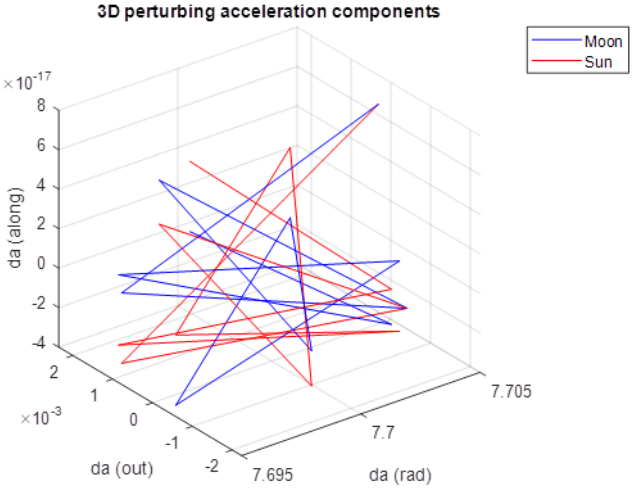

Figure (8): Acceleration components directions during perturbation on retrograde Low Earth Orbit satellite (LEO).

The perturbation effects on accelerations in three directions (radial, along-track, and out of plane) are shown in figures (7) and (8). The results show that the effects of the sun and the moon on radial and out of plane direction is periodic and tiny range of influence so on acceleration components for low-altitude satellites are identical and small, but along direction has a different effect.

9. Conclusion

This work examined the effects of third-body perturbation (moon, sun) on LEO orbit satellites for retrograde and prograde orbit. We determined that the moon and the sun had the same influence on the motion of the satellites by comparing their effects on the component of geocentric equatorial coordinates and orbital elements, so on Kepler's orbit and acceleration components. The third body does not have recognized influence in the orbits near the atmosphere of Earth at an altitude below 1000 km which be more influenced by Drag force and radiations force as much as the orbits move through an altitude of below 1000 km more than this range of heights third body has grater effects seen in high orbits as geostationary, GPS and earth observation satellites.

When the effects of the moon and the sun are compared, the impacts on the out of plane acceleration components are different. However, because of the two planets' influences, there is a

divergence in the perturbed orbits component regarding osculating orbits. Prograde orbits were more influenced than retrograde orbits in the radial and along direction components, but retrograde orbits seemed more impacted in the other component.

REFERENCES

1. E. 2000- 2022, "eoportal directory," 2022. https://directory.eoportal.org/web/eoportal/satellite-missions/m/meteor-m-2.
2. david A. Vallado, FUNDAMENTALS OF ASTRODYNAMICS AND APPLICATIONS, Fourth Edi. Published jointly by Microcosm Press and Springer, 2013.
3. L. Rogres, It's only rocket Science. © 2008 Springer Science+Business Media, LLC, 2008.
4. W. Torge and J. Müller, Geodesy, 4th Editio. © 2012 Walter de Gruyter GmbH & Co. KG, Berlin/Boston.
5. G. Seeber, Satellite Geodesy, 1 st editi. Copyright 2003 by Walter de Gruyter GmbH & Co. KG,10785 Berlin, 2003.
6. G. X. • J. Xu, Orbits, Second Edi. # Springer-Verlag Berlin Heidelberg 2013, 2013.
7. Y. Kozai, "The motion of a close earth satellite," Astron. J., vol. 64, p. 367, 1959, doi: 10.1086/107957.
8. Yoshihide kozai, "A NEW METHOD TO COMPUTE LUNISOLAR PERTURBATIONS IN SATELLITE MOTIONS," Smithson. Astrophys. Obs., 1973.
9. Martin Lara · Juan F. San-Juan · Luis M. López and P. J. Cefola, "On the third-body perturbations of high-altitude orbits," Celest Mech Dyn Astr, 2012.
10. C. W. T. R. · S. R. V. and K. T. Alfriend2, "Third-Body Perturbation Effects on Satellite Formations," J Astronaut Sci, 2015.

    B. De Saedeleer, "Analytical theory of a lunar artificial satellite with third body perturbations," Celest. Mech. Dyn. Astron., 2006.
11. G. B. · A. J. · U. H. · L. Mervart, "Efficient satellite orbit modelling using pseudo-stochastic parameters," J. Geod., 2006, doi: 10.1007/s00190-006-0072-6.
12. Guangyan Xua, J. Luo, Z. Li, and X. Chen, "Equations of Satellite Relative Motion in Low Earth Orbit under Lunar Perturbation," Proc. 2014 IEEE Chinese Guid. Navig. Control Conf., 2014.
13. E. D. Kuznetsov and A. T. Jasim, "On the Long_Period Evolution of the Sun_Synchronous Orbits," Sol. Syst. Res., vol. 50, no. 3, 2015, doi: 10.1134/S0038094616030059.
14. A. K. Izzet, M. J. Hamwdi, and A. T. Jasim, "Analytical Study of Earth Tides on Low Orbits Satellites," Iraqi J. Sci., vol. 61, no. 2, pp. 453–461, 2019, doi: 10.24996/ijs.2020.61.2.252.
15. S. U. Yazan Chihabi ∗, "Analytical spacecraft relative dynamics with gravitational, drag and third-body perturbations," Acta Astronaut., 2021, doi: 10.1016/j.actaastro.2021.04.043.
16. Y. Du, Fangzhao Zhang, T. Xu, F. Gao, and G. Xu, "Correction of precession-nutation and polar motion in analytical solutions of satellite equations of motion," Adv. Sp. Res., 2021, doi: 10.1016/j.asr.2021.07.041.
17. N. O. Hasan, W. H. A. Zaki, and A. K. Izzet, "The Effect of Atmospheric Drag Force on the Elements of Low Earth Orbital Satellites at Minimum Solar Activity," NeuroQuantology, vol. 19, no. 9, pp. 24–37, 2021, doi: 10.14704/nq.2021.19.9.NQ21134.
18. E. M. Alessi, A. Buzzoni, J. Daquin, A. Carbognani, and G. Tommei, "Dynamical properties of the Molniya satellite constellation: Long-term evolution of orbital eccentricity," Acta Astronaut., pp. 659–669, 2021, doi: 10.1016/j.actaastro.2020.11.047.
19. V. A. Chobotov, Orbital Mechanics, Third Edit. American Institute of Aeronautics and Astronautics, Inc., 2002.
20. M. Capderou, Satellites Orbits and Missions. © Springer-Verlag France 2005, 2005.
21. G. Beutler, Methods of Celestial Mechanics Volume II: Springer-Verlag Berlin Heidelberg 2005, 2005.
22. [23] G. X. • Y. Xu, GPS, Third Edit. © Springer-

Verlag Berlin Heidelberg, 2016.

23. [24] P. Gurfil, Modern Astrodynamics, First edit. 2006, Elsevier Ltd. All rights reserved, 2006.
24. [25] G. Beutler, Methods of Celestial Mechanics Volume I: © Springer-Verlag Berlin Heidelberg 2005.